

# ACP-OPLL Photonic Integrated Circuits for High Dynamic Range RF/Photonic links

<sup>a\*</sup>Yifei Li, <sup>b</sup>Ashish Bhardwaj, <sup>b</sup>Larry Coldren, <sup>b</sup>John Bowers, and <sup>c</sup>Peter Herczfeld  
<sup>a</sup>ECE Dept, UMass Dartmouth, 285 Old Westport RD, Dartmouth, MA, USA 02747;  
<sup>b</sup>ECE Dept, The Univ. of California Santa Barbara, Santa Barbara, CA, USA 93106;  
<sup>c</sup>ECE Dept, Drexel Univ, 3100 Market street, Philadelphia, PA USA 19104

## ABSTRACT

Fiber-optic links are attractive for transmitting microwave/millimeter wave signals for applications such as radar, imaging and astronomy. However, current fiber-optic links that employ intensity modulation and direct detection suffer from limited spurious free dynamic range (SFDR). For solution, a new coherent fiber-optic link using linear phase modulation/demodulation has been proposed. The new link should be able to achieve an SFDR two orders of magnitude higher. The key for this link is an Optical Phase Locked Loop (OPLL) linear phase demodulator. In this paper we describe the design and preliminary measurements for the first generation ACP-OPLL photonic integrated circuits.

**Keywords:** optical phase locked loop, photonic integrated circuits, RF/Photonic link, and dynamic range

## 1. INTRODUCTION

Fiber-optic links are attractive for front-end applications due to their low loss, lightweight flexible cabling, immunity to electromagnetic interference, broad bandwidth, and low loss. Unlike conventional optical links for data communications, fiber-optic links in front-end applications require a large spurious free dynamic range (SFDR). Existing fiber-optic links employ intensity modulation and direct detection by a photodetector. Although simple, they have limited dynamic range due to the inherent nonlinearities in the optical intensity modulators. The state-of-the-art optical links manage to achieve an SFDR in the range of  $115 \text{ dB}\cdot\text{Hz}^{2/3}$  through extensive linearization techniques [1]. However, many critical applications (such as channelized electronic warfare receivers) require an SFDR in excess of  $140 \text{ dB}\cdot\text{Hz}^{2/3}$ .

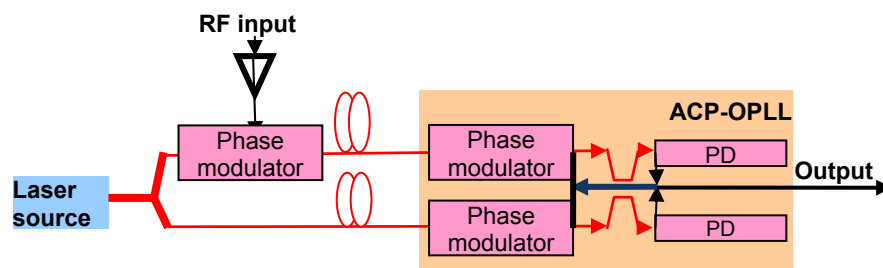


Fig. 1: RF/photonic link employing an ACP-OPLL phase demodulator

We have proposed a coherent, phase modulated RF/photonic link shown in Fig. 1 [2-3]. The most critical element in this approach is a linear optical phase locked loop (OPLL) linear phase demodulator. Through feedback, the OPLL forces the phase of a local phase modulator to mirror the phase of an incoming optical signal. Thus, the output from the photodetector is a scaled replica of the RF input. In order to tightly track the in-coming optical phase, the OPLL must have a high open loop gain ( $\sim 20 \text{ dB}$ ) and a wide bandwidth ( $> 0.5 \text{ GHz}$ ). Feedback stability requires that the OPLL has an extremely short feedback loop propagation delay ( $< 8 \text{ ps}$ ). We have shown that an OPLL that is based on an attenuation counter-propagating (ACP) design [4] provides a lumped-element response to both the local optical phase modulators

and the photodetectors inside the OPLL. To further reduce the loop delay, the components of the ACP-OPLL should be integrated to form a photonic integrated circuit (PIC).

## 2. ACP-OPLL PIC DESIGN

A schematic view of an ACP-OPLL PIC is shown in Fig. 2. It contains a pair of balanced ACP local optical phase modulator, a pair of counter-propagating balanced photodetectors, a 3dB optical coupler and a feedback trace from the photodetector common electrode to the phase modulator common electrode. Through phase tracking the OPLL forces the optical phase of the local ACP phase modulator to mirror that of the incoming optical phase. Next, we discuss the design of the loop components that are used to fabricate an ACP-OPLL PIC.

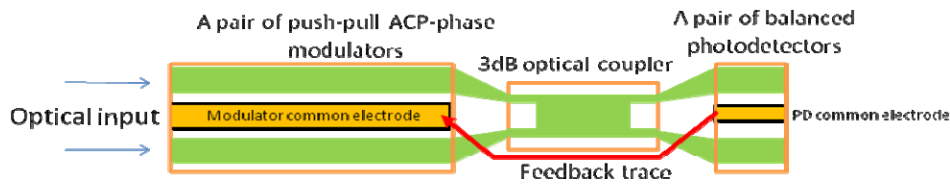


Fig. 2: Schematic of an ACP-OPLL PIC

### 2.1 MQW ACP optical phase modulator pair

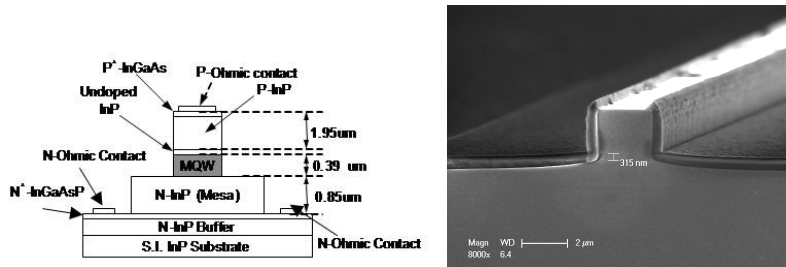


Fig. 3: Device structure for the InP MQW Phase modulator

The ACP-OPLL PIC employs InGaAsP-based multi-quantum wells (MQW) to realize optical phase modulators. However, in general the MQW phase modulators exhibit unwanted nonlinearities and electroabsorption, leading to high optical propagation losses. Both of these effects can limit the performance of the OPLL linear phase demodulator. To overcome this problem, we developed a detuned shallow quantum well optical phase modulator structure [5] (see Fig. 3). The quantum well region consists of lattice matched 9 nm thick  $\text{In}_{0.65}\text{Ga}_{0.35}\text{As}_{0.76}\text{P}_{0.24}$  quantum wells and 6.5 nm thick  $\text{In}_{0.8}\text{Ga}_{0.2}\text{As}_{0.44}\text{P}_{0.56}$  barriers. To reduce the absorption in the quantum wells, the quantum well photoluminescence (PL) peak is designed to be  $\sim 170$  nm away from the  $1.55 \mu\text{m}$  operating wavelength. To reduce free carrier optical absorption, a low barrier height is used to help with sweeping out the photo-generated carriers. The low barrier height also reduces the quantum confinement at high reverse bias voltages. In general, the PM sensitivity of a quantum well phase modulator increases with the bias voltage. The reduction of the quantum confinement can diminish the PM sensitivity increase. Thus, near a certain reverse bias, this helps to create a plateau region where the PM sensitivity held constant against the bias voltage change. In this region, the phase modulator will behave more linear. The phase modulator device structure has a p-i-n diode configuration. To improve the lateral confinement, a deep ridge waveguide structure is used. The intrinsic region contains 25 periods of quantum wells, yielding a confinement factor of 0.63 when the quantum wells act as the guiding layer of the deep ridge waveguide structure. The width of the optical waveguide is  $2 \mu\text{m}$ . At a reverse bias of 6 V, a 1 mm long phase modulator device demonstrated:

- Large phase modulation linearity:  $\phi_{IP3} \sim 4\pi$  @ 6 volt bias
- Low insertion loss:  $\sim 0.9\text{dB}$  @ 6 volt bias
- $V_{\pi}$ :  $\sim 6\text{V}$  @ 6 volt bias

This quantum well design is used to implement the phase modulators in the ACP-OPLL PICs. To meet the SFDR goal of  $140 \text{ dB}\cdot\text{Hz}^{2/3}$ , the combined  $\phi_{IP3}$  of the ACP phase modulator should be over  $20\pi$  [x]. Therefore, 3 mm long phase modulator length were chosen. A pair of 3mm long phase modulators in a push-pull configuration should yields a combined  $\phi_{IP3}$  of  $24\pi$ .

The ACP configuration eliminates the phase delay from the phase modulators. The ACP phase modulators require that RF attenuation is applied to the modulator electrode. This is accomplished by employing high resistance electrodes ( $\sim 150 \text{ ohm}$ ) to both the n and p contacts of the phase modulator pair. Fig. 3 shows the simulated response of the push-pull ACP-phase modulator pair. The simulated phase modulation sensitivity is  $\sim 3.2 \text{ rad/volt}$ , which corresponds to a  $V_{\pi}$  of  $\sim 1 \text{ V}$ . Its 3-dB bandwidth is  $\sim 0.5 \text{ GHz}$ . In addition, as shown in Fig. 4b, the phase response of the ACP phase modulator pair is bound between 0 and  $\pi/2$ . This suggests that a lumped element response that would result in the absence of phase delay in the feedback loop. The simulated ACP phase modulator load impedance is also shown in Fig. 5. To help increase the OPLL open loop gain, a high modulator load impedance is desired.

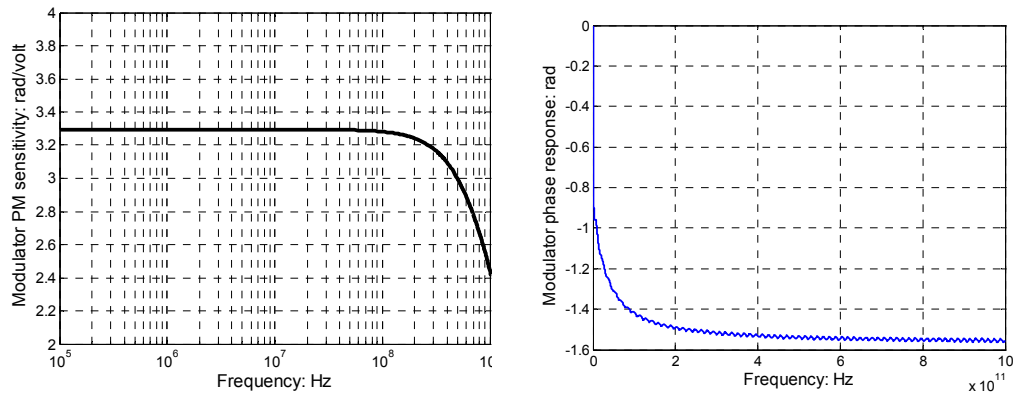


Fig. 4: Phase modulator frequency response.

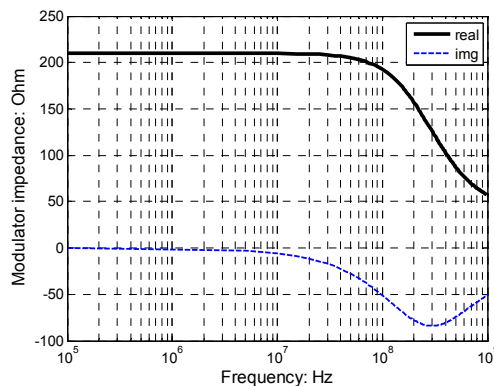


Fig. 5 Load impedance of the ACP-phase modulator pair

## 2.2 Balanced photodetector

We use the waveguide uni-traveling carrier waveguide photodiode (UTC) design developed by Klamkin et al [6] as the basis to implement the balanced photodetectors for the ACP-OPLL photonic integrated circuit. However, we employ a counter-propagating photodetection scheme to help mitigate the phase delay of the photodetectors[7]. In this configuration, the optical field counter-propagates with respect to the photo-generated feedback signal. The width and the total length of the photodetector waveguides are 10 microns and 200 microns, respectively. Fig. 5 shows the simulated response of the photodetector when the balanced photodetector is loaded by the ACP-phase modulator pair and an external load (50 ohm or 150 ohm). The frequency response is defined as the ratio between the photodetector output voltage and the optical input power. A lower load impedance will result in a larger photodetection bandwidth (~2GHz), whereas a higher impedance will result in a higher output voltage.

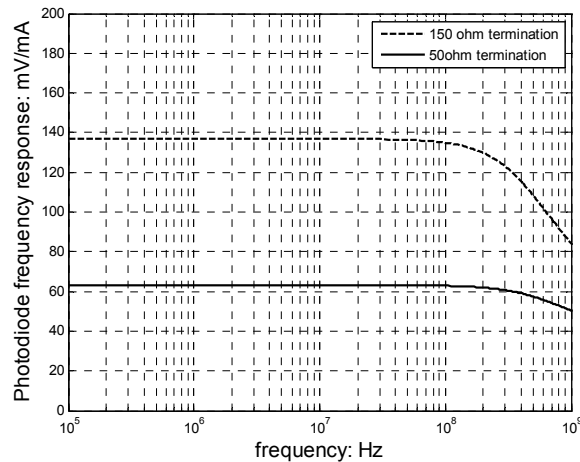


Fig. 6: Frequency response of counter propagating balanced UTC photodetector when loaded by a pair of 3mm long ACP local phase modulators in parallel with an external termination.

## 2.3 Optical 3dB coupler

In order to implement a compact 3-dB optical 2x2 coupler, a regular multi-mode interferometric (MMI) coupler is designed. The width of the MMI section is 7 microns and the length of the coupler is 219 microns.

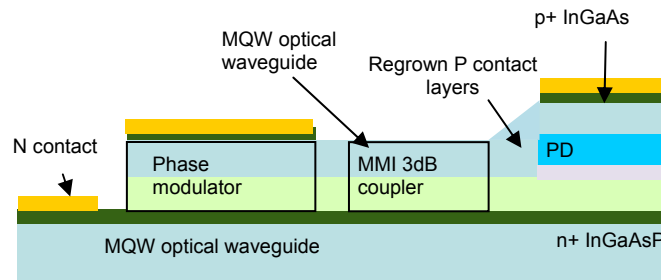


Fig. 7: Monolithic integration platform for the fabrication of the ACP-OPLL PIC

## 2.4 ACP-OPLL PIC designs

The monolithic integration platform used for the ACP local phase modulators, the UTC-photodetectors, and the 3-dB 2x2 coupler is shown in Fig. 7. The phase modulators and the photodetectors are connected by a regular multi-mode interferometric (MMI) 3dB optical coupler. The length of the MMI coupler and the electric feedback path results in the

total loop delay of the ACP-OPLL loop delay to be  $\sim 10$  ps. The three variations of the ACP-OPLL PICs were designed and implemented (see Fig. 8). They are: the ACP-OPLL with 3 mm long modulators, the ACP-OPLL with 2.2 mm long modulators, and an optoelectronic ACP-OPLL. The optoelectronic ACP-OPLL, which also has 2.2 mm long ACP phase modulators, can be hybrid-integrated with an electronic amplifier circuit in order to increase the OPLL open loop gain.

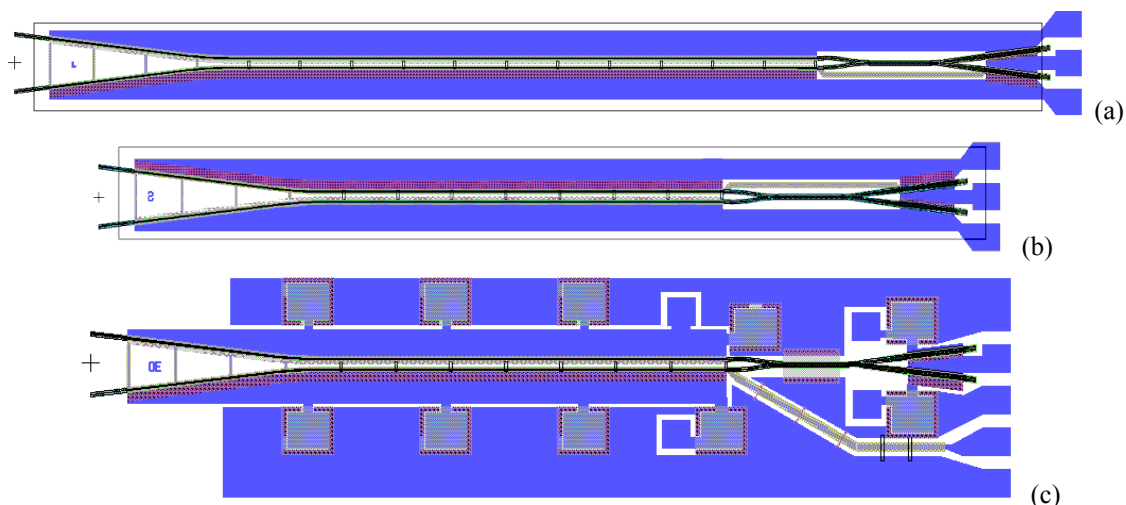


Fig. 8: Three designs of ACP-OPLL PICs. (a) ACP-OPLL with 3 mm phase modulator; (b) ACP-OPLL with 2.2 mm phase modulator; (c) optoelectronic ACP-OPLL with 2.5 mm long phase modulator

### 3. ACP-OPLL PIC CHARACTERIZATION- PRELIMINARY RESULTS

The ACP-OPLL PICs were fabricated using the nanofabrication facilities at UCSB. In this section, we present some preliminary experimental results from the ACP-OPLL PICs with the 3 mm long ACP-modulators. Fig. 9 shows a group of three ACP-OPLL PICs being probed. The experimental setup for characterizing the ACP-OPLL was depicted in Fig. 10.

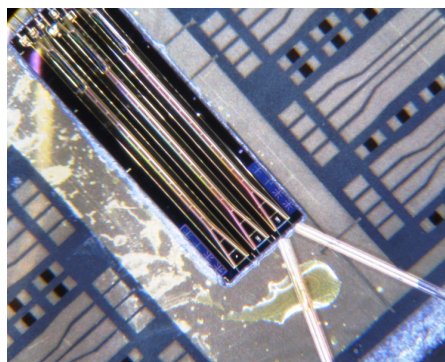


Fig. 9: ACP-OPLL PIC characterization

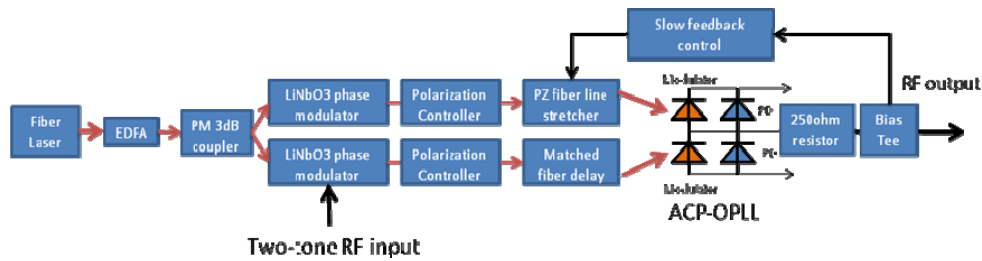


Fig. 10: PM link experimental setup

In this set of measurements, a 250ohm series resistor was placed between the ACP-OPLL output and the external 50 ohm load. This increases the ACP-OPLL open loop gain but it is at expense of the OPLL bandwidth, but ensures adequate voltage drop across the phase modulators. Phase tracking is clearly observed in the ACP-OPLL PIC. As shown in Fig. 11, with only 4mA photocurrent, we observed a **21dB** improvement in intermodulation distortion. Figure 12 shows the OPLL output and spurious distortion level when the RF input power is swept from 12 to 14dBm. The distortion level follows strictly 3:1 slope and the link input IP3 point is 39dBm.

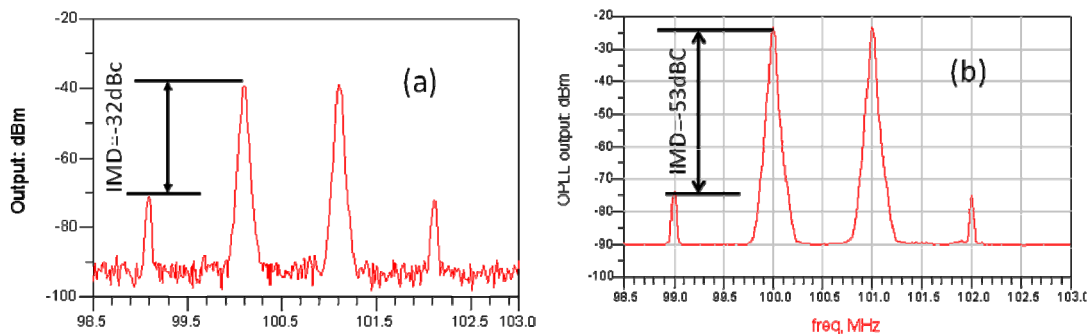


Fig. 11: Comparison of inter-modulation distortion levels between the ACP-OPLL (LW1) and an conventional homodyne phase detector. (a). Output spectrum of a conventional homodyne phase detector ; (b) Output spectrum of the ACP-OPLL. RF input is 14dBm/tone in both cases. The photocurrent of the ACP-OPLL is ~4mA and the bias is 6V.

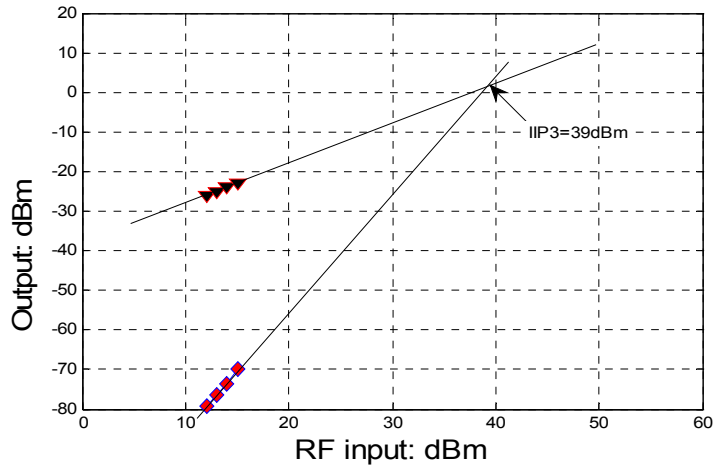


Fig. 12: Output vs RF input

#### 4. CONCLUSION

In this paper we have described the design and preliminary experimental results for an ACP-OPLL photonic integrated circuit that can be used as a linear optical phase demodulator in high dynamic range RF/photonic links. Phase demodulation by phase tracking has been observed.

#### REFERENCES

- [1] E.I. Ackerman, "Broad-band linearization of a Mach-Zehnder electro-optic modulators", IEEE Trans. Microwave Theory and Tech., Vol. 47, pp 2271-2279, Dec. 1999
- [2] J. E. Bowers, A. Ramaswamy, L.A. Johansson, J. Klamkin, M.N. Sysak, D.Zibar, L.A. Coldren, M.J. Rodwell, L. Lembo, R. Yoshimitsu, D. Scott, R. Davis, P. Ly, "Linear Coherent Receiver based on a Broadband and Sampling Optical Phase-Locked Loop," Microwave Photonics '07 (Invited), Victoria, Canada, OCTOBER 2007
- [3] Y. Li, P. Herczfeld, "Coherent PM optical link employing ACP-PPLL", OSA/IEEE Journal of Lightwave Technology, vol. 27, no. 9, May 2009, pp. 1086-1094.
- [4] Y. Li, P. Herczfeld, "Novel attenuation counter propagating phase modulator for highly linear fiber optic links", OSA/IEEE Journal of Lightwave Technology, Oct., 2006
- [5] Y. Li, R. Wang, A. Bhardwaj, S. Ristic and J. Bowers, "High linearity InP based phase modulators using a Shallow Quantum well Design", IEEE Photonic Technology Letter, vol 22, no. 18, 2010, pp 1340-1342
- [6] J. Klamkin, et al, "Output Saturation and Linearity of Waveguide Unitraveling-Carrier Photodiodes," IEEE Journal of Quantum Electronics, 44, (4), pp. 354-359, April 2008
- [7] Y. Li, R. Wang, J. Klamkin, S. Madison, P. Juodawlkis, P. Herczfeld and J. Bowers, "Delay of counter-propagating photodiodes", IEEE/OSA Journal of Lightwave Technology, vol. 28, no. 15, 2010, pp 2099-2104.